SUPPLEMENTARY INFORMATION

Diruthenium complexes as pH-responsive delivery systems: a quantitative assessment

Isabel Coloma,[a] Miguel Cortijo,*[a] María José Mancheño,[b] María Eugenia León-González,[c] Crisanto Gutierrez,[d] Bénédicte Desvoyes,*[d] and Santiago Herrero*[a]

[a.] *Inorganic Chemistry Department, Faculty of Chemistry, Universidad Complutense de Madrid, E-28040 Madrid, Spain.*
[b.] *Organic Chemistry Department, Faculty of Chemistry, Universidad Complutense de Madrid, E-28040 Madrid, Spain*
[c.] *Analytical Chemistry Department, Faculty of Chemistry, Universidad Complutense de Madrid, E-28040 Madrid, Spain*
[d.] *Centro de Biología Molecular Severo Ochoa, CSIC-UAM, E-28049 Madrid, Spain.*

1. SINGLE CRYSTAL X-RAY DIFFRACTION

- Table S1. Crystal and structure refinement data for **Ru'2,4-D**

- Figure S1. Asymmetric unit of **Ru'2,4-D**

- Figure S2. Intra- and intermolecular interactions found in the structure of **Ru'2,4-D**

- Table S2. Selected bond distances and angles for **Ru'2,4-D**

- Table S3. Crystal and structure refinement data for **Ru'NAA**

- Figure S3. Intermolecular interactions found in the structure of **Ru'NAA**

- Table S4. Selected bond distances and angles for **Ru'NAA**

2. MASS SPECTROMETRY

- Figure S4. ESI$^+$ spectra of **Ru'IAA**, **Ru'2,4-D** and **Ru'NAA**

- Figure S8. ESI$^-$ analyses of **Ru'2,4-D** and **Ru'2,4-D** after 24 h at pH = 6.5

3. IR SPECTROSCOPY

- Figure S5. IR spectra of $[Ru_2Cl(\mu\text{-DAniF})_3(\mu\text{-O}_2CMe)]$, $[Ru_2Cl_2(\mu\text{-DAniF})_3]$, **Ru'IAA**, **Ru'2,4-D** and **Ru'NAA**

- Table S5. Tentative assignment of the most relevant bands in the IR spectra of $[Ru_2Cl(\mu\text{-DPhF})_3(\mu\text{-O}_2CMe)]$, $[Ru_2Cl(\mu\text{-DAniF})_3(\mu\text{-O}_2CMe)]$, $[Ru_2Cl_2(\mu\text{-DPhF})_3]$, $[Ru_2Cl_2(\mu\text{-DAniF})_3]$, **RuIAA**, **Ru2,4-D**, **RuNAA**, **Ru'IAA**, **Ru'2,4-D** and **Ru'NAA**

4. ELECTRONIC SPECTROSCOPY

- Figure S6. Electronic spectra of $[Ru_2Cl(\mu\text{-DAniF})_3(\mu\text{-O}_2CMe)]$, **Ru'IAA**, **Ru'2,4-D**, **Ru'NAA** and $[Ru_2Cl(\mu\text{-DPhF})_3(\mu\text{-O}_2CMe)]$

- Table S6. Tentative assignment of the transitions observed in the electronic spectra of $[Ru_2Cl(\mu\text{-DPhF})_3(\mu\text{-O}_2CMe)]$, **RuIAA**, **Ru2,4-D**, **RuNAA**, $[Ru_2Cl(\mu\text{-DAniF})_3(\mu\text{-O}_2CMe)]$, **Ru'IAA**, **Ru'2,4-D** and **Ru'NAA**

5. MAGNETIC MEASUREMENTS

6. BIOLOGICAL ASSAYS AND CHEMOMETRICS

1. SINGLE CRYSTAL X-RAY DIFFRACTION

Table S1. Crystal and structure refinement data for **Ru'2,4-D**.

|	
Empirical formula	$C_{53}H_{50}Cl_3N_6O_9Ru_2$
Formula weight	1223.48
Temperature/K	296.15
Crystal system	triclinic
Space group	P-1
a/Å	11.869(2)
b/Å	15.027(3)
c/Å	16.745(3)
α/°	101.077(4)
β/°	107.283(3)
γ/°	106.402(3)
Volume/Å³	2608.4(8)
Z	2
ρ_{calc}g/cm³	1.558
μ/mm⁻¹	0.795
F(000)	1242.0
Crystal size/mm³	0.34 × 0.2 × 0.07
Radiation	MoKα (λ = 0.71073)
2Θ range for data collection/°	2.672 to 50.698
Index ranges	-14 ≤ h ≤ 14, -18 ≤ k ≤ 18, -20 ≤ l ≤ 20
Reflections collected	22965
Independent reflections	9497 [R_{int} = 0.0774, R_{sigma} = 0.1203]
Data/restraints/parameters	9497/0/664
Goodness-of-fit on F²	0.971
Final R indexes [I>=2σ (I)]	R_1 = 0.0547, wR_2 = 0.1162
Final R indexes [all data]	R_1 = 0.1270, wR_2 = 0.1498
Largest diff. peak/hole / e Å⁻³	0.96/-0.61
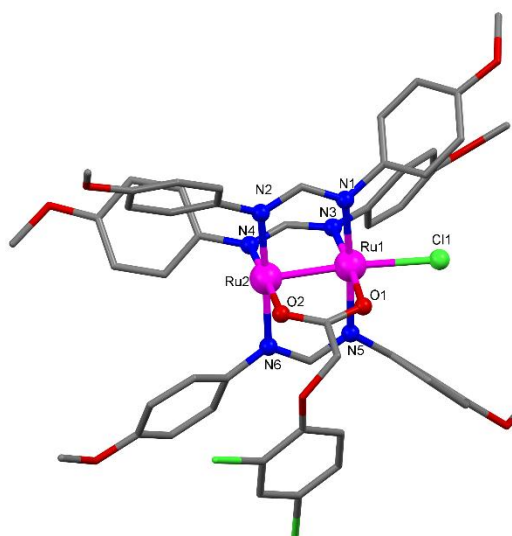
Figure S1. Asymmetric unit of **Ru'2,4-D**. Hydrogen atoms are omitted for clarity.
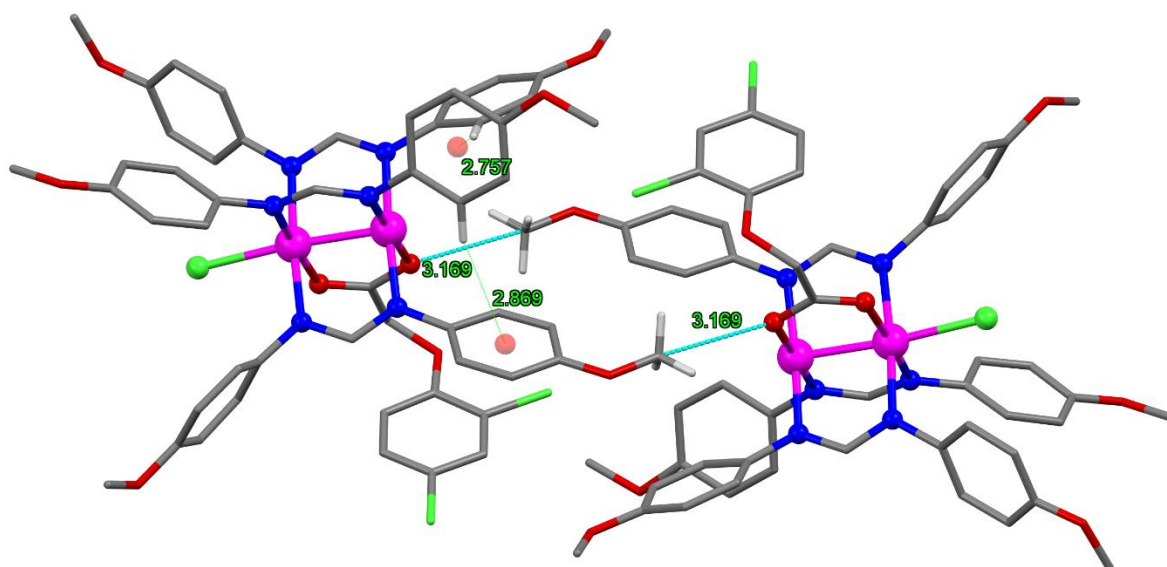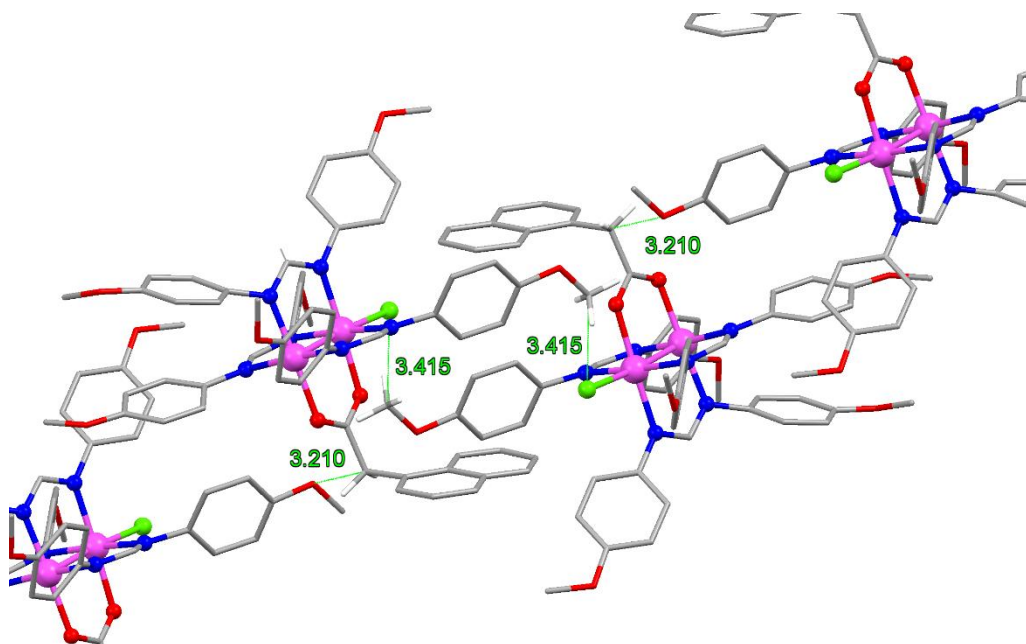
Figure S2. Intra- and intermolecular interactions found in the structure of of **Ru'2,4-D** (distances in Å).

Table S2. Selected bond distances (Å) and angles (deg) for **Ru'2,4-D**.

Ru1	Ru2	2.3288(8)	
Ru1	Cl1	2.416(2)	
Ru1	O1	2.113(5)	
Ru1	N1	2.096(5)	
Ru1	N3	2.060(6)	
Ru1	N5	2.102(5)	
Ru2	O2	2.068(5)	
Ru2	N2	2.044(6)	
Ru2	N4	2.005(6)	
Ru2	N6	2.029(5)	
Ru1	Ru2	Cl1	173.69(5)
Ru1	O1	N3	176.1(2)
Ru1	N1	N5	175.7(2)
Ru2	O2	N4	178.4(2)
Ru2	N2	N6	174.5(2)

Table S3. Crystal and structure refinement data for **Ru'NAA**.

|	
Empirical formula	$C_{57}H_{54}ClN_6O_8Ru_2$
Formula weight	1188.65
Temperature/K	100.0
Crystal system	triclinic
Space group	P-1
a/Å	10.3478(4)
b/Å	16.5979(7)
c/Å	16.8204(8)
α/°	110.212(2)
β/°	91.855(2)
γ/°	104.522(2)
Volume/Å³	2601.8(2)
Z	2
$\rho_{calc}g/cm^3$	1.517
μ/mm^{-1}	5.678
F(000)	1214.0
Crystal size/mm³	0.21 × 0.04 × 0.02
Radiation	CuKα (λ = 1.54178)
2Θ range for data collection/°	5.648 to 136.49
Index ranges	-11 ≤ h ≤ 12, -19 ≤ k ≤ 19, -20 ≤ l ≤ 20
Reflections collected	99612
Independent reflections	9537 [R_{int} = 0.1196, R_{sigma} = 0.0536]
Data/restraints/parameters	9537/0/673
Goodness-of-fit on F²	1.041
Final R indexes [I>=2σ (I)]	R_1 = 0.0524, wR_2 = 0.1112
Final R indexes [all data]	R_1 = 0.0854, wR_2 = 0.1338
Largest diff. peak/hole / e Å⁻³	2.55/-1.03

Figure S3. Intermolecular interactions found in the structure of **Ru'NAA** (distances in Å).

Table S4. Selected bond distances (Å) and angles (deg) for **Ru'NAA**.

Ru1	Ru2	2.3155(6)	
Ru1	Cl1	2.395(1)	
Ru1	O1	2.079(4)	
Ru1	N1	2.107(5)	
Ru1	N3	2.083(4)	
Ru1	N5	2.091(5)	
Ru2	O2	2.066(4)	
Ru2	N2	2.046(4)	
Ru2	N4	2.024(4)	
Ru2	N6	2.039(5)	
Ru1	Ru2	Cl1	173.92(4)
Ru1	O1	N3	177.0(2)
Ru1	N1	N5	175.5(2)
Ru2	O2	N4	178.5(2)
Ru2	N2	N6	176.2(2)

2. MASS SPECTROMETRY
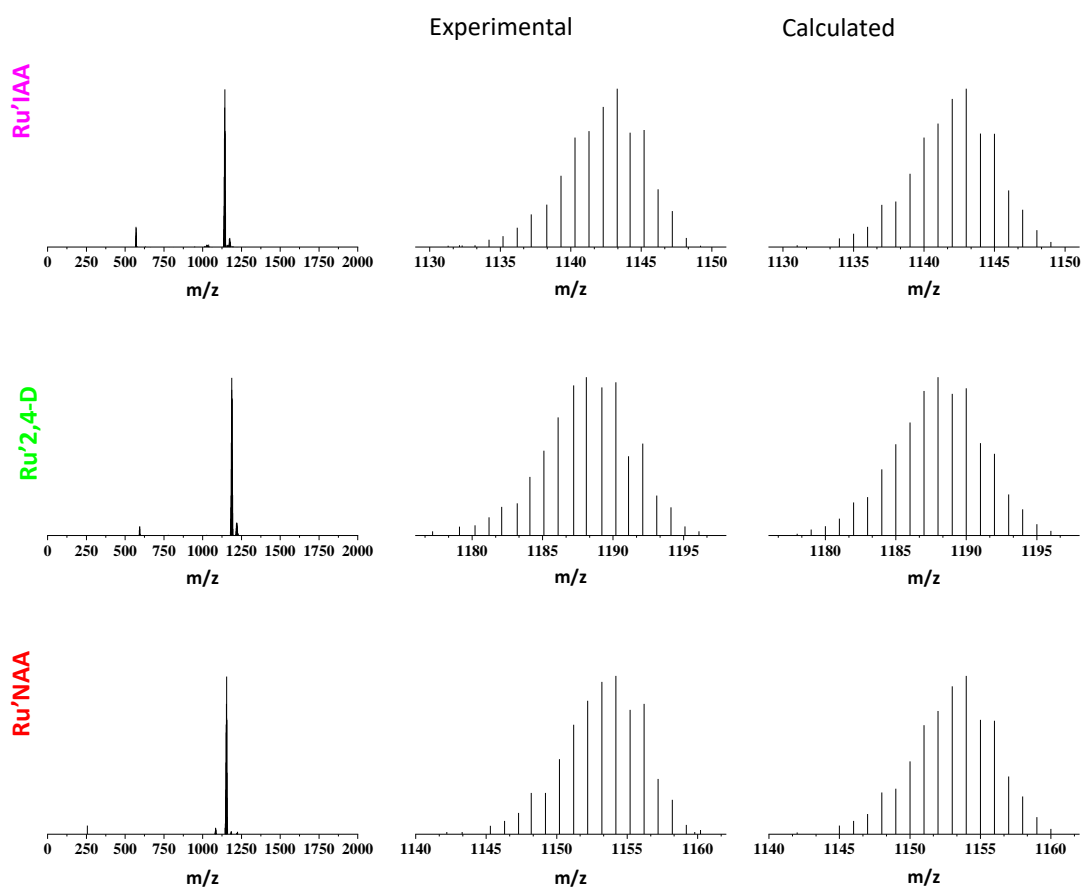
Figure S4. ESI[+] spectra of **Ru'IAA**, **Ru'2,4-D** and **Ru'NAA** (left). Enlargement of the peak corresponding to [M-Cl][+] base peak (centre) and calculated spectra for the [M-Cl][+] fragments (right) of **Ru'IAA** (top), **Ru'2,4-D** (middle) and **Ru'NAA** (bottom). Nominal molecular masses and distribution isotopes were calculated with the MASAS[1] software.

---

[1] F. A. Urbanos. Software MASAS, Universidad Complutense de Madrid: Madrid, 2002.
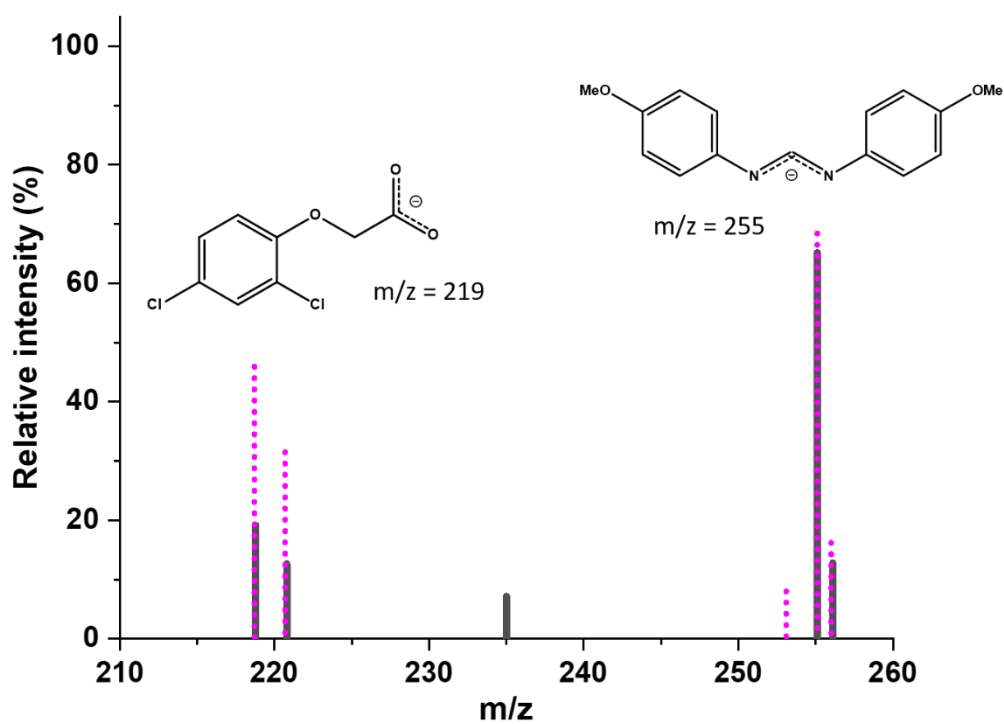
Figure S8. ESI⁻ analyses of **Ru'2,4-D** (black) and **Ru'2,4-D** after 24 h at pH = 6.5 (pink). Both samples were dissolved in methanol. The second one was slightly acidified with HCl keeping the pH at 6.5. The intensities of both spectra were normalized to their base peak, which is the same in both cases.

3. IR SPECTROSCOPY
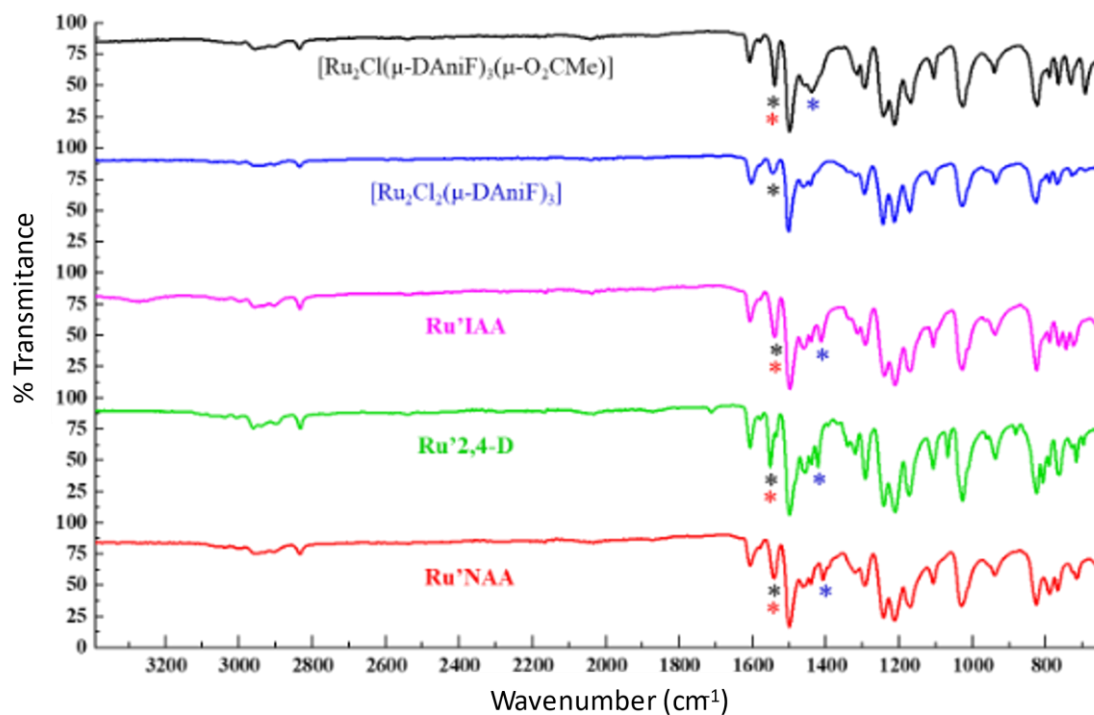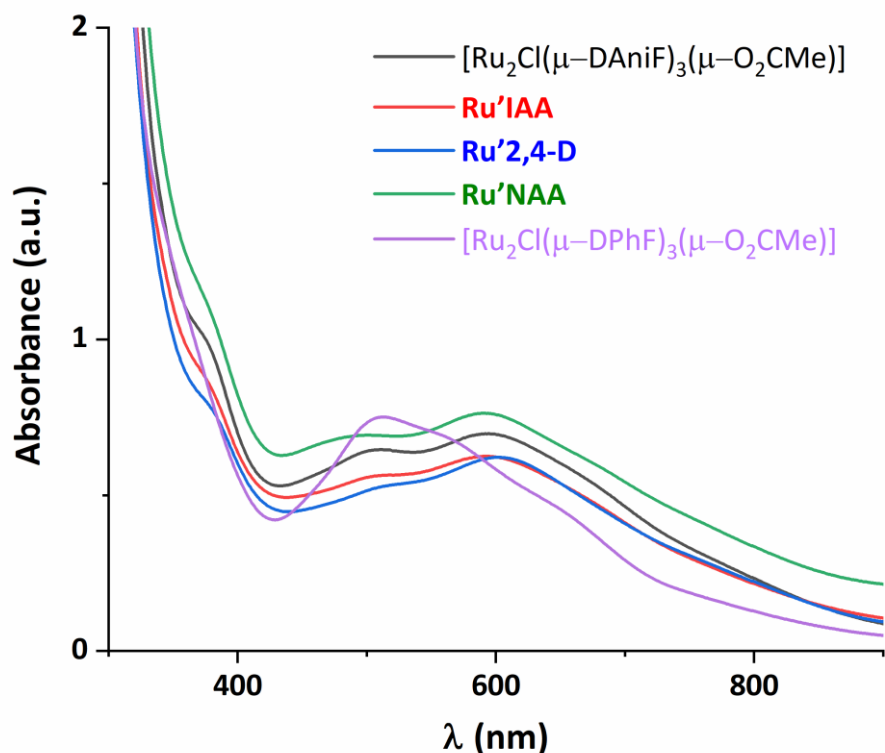

Figure S5. IR spectra of [Ru$_2$Cl(μ-DAniF)$_3$(μ-O$_2$CMe)] (black), [Ru$_2$Cl$_2$(μ-DAniF)$_3$] (blue), **Ru'IAA** (pink), **Ru'2,4-D** (blue) and **Ru'NAA** (red). The antisymmetric O-C-O stretching bands are marked with a red asterisk, the symmetric O-C-O stretching bands with a blue asterisk and the N-C-N stretching bands with a black asterisk.

Table S5. Tentative assignment of the most relevant bands (cm^{-1}) in the IR spectra of [Ru$_2$Cl(μ-DPhF)$_3$(μ-O$_2$CMe)], [Ru$_2$Cl(μ-DAniF)$_3$(μ-O$_2$CMe)], [Ru$_2$Cl$_2$(μ-DPhF)$_3$], [Ru$_2$Cl$_2$(μ-DAniF)$_3$], **RuIAA**, **Ru2,4-D**, **RuNAA**, **Ru'IAA**, **Ru'2,4-D** and **Ru'NAA**.

Compound	ν N-H	ν C$_{ar}$-H	ν$_{as}$ C-H	ν$_s$ C-H	ν C=C$_{ar}$	ν$_{as}$ O-C-O + ν N-C-N	ν$_s$ O-C-O	ν C-N	Δ (ν$_{as}$ - ν$_s$ O-C-O)
[Ru$_2$Cl(μ-DPhF)$_3$(μ-O$_2$CMe)]	-	3057	2957	-	1592 1485	1529	1430	1308 1211	99
[Ru$_2$Cl(μ-DAniF)$_3$(μ-O$_2$CMe)]	-	3005	2957	2835	1607 1578 1484	1540	1438	1292 1212	102
[Ru$_2$Cl$_2$(μ-DPhF)$_3$]	-	3063	2951	-	1591 1582 1484	1520*	-	1312 1208	-
[Ru$_2$Cl$_2$(μ-DAniF)$_3$]	-	3042	2944	2834	1602 1498	1539*	-	1294 1210	-
RuIAA	3260	3056	2965	-	1595 1485	1530	1408	1317 1214	122
Ru2,4-D	-	3060	2968	-	1592 1486	1547	1426	1317 1219	121
RuNAA	-	3056	2954	-	1593 1486	1531	1408	1318 1220	123
Ru'IAA	3276	3039	2957	2833	1606 1497	1540	1412	1291 1239	138
Ru'2,4-D	-	3039	2959	2832	1606 1497	1551	1421	1291 1210	130
Ru'NAA	-	3036	2954	2833	1606 1499	1541	1407	1292 1212	134

*Corresponds only to ν$_{as}$ O-C-O.

4. ELECTRONIC SPECTROSCOPY

Figure S6. Electronic spectra of [Ru$_2$Cl(μ-DAniF)$_3$(μ-O$_2$CMe)] (black), **Ru'IAA** (red), **Ru'2,4-D** (blue), **Ru'NAA** (green) and [Ru$_2$Cl(μ-DPhF)$_3$(μ-O$_2$CMe)] (purple).

Table S6. Tentative assignment, of the transitions (nm) observed in the electronic spectra of [Ru$_2$Cl(μ-DPhF)$_3$(μ-O$_2$CMe)], **RuIAA**, **Ru2,4-D**, **RuNAA**, [Ru$_2$Cl(μ-DAniF)$_3$(μ-O$_2$CMe)], **Ru'IAA**, **Ru'2,4-D** and **Ru'NAA**.[2]

Transition	LMCT π(Cl)→π*(Ru$_2$)	π(RuO/N,Ru$_2$)→ π*(Ru$_2$)	π*(Ru$_2$)→ σ*(RuO/N)	δ(Ru$_2$)→ π*(Ru$_2$)
[Ru$_2$Cl(μ-DPhF)$_3$(μ-O$_2$CMe)]	340 sh	515	565 sh	665 sh
RuIAA	335 sh	517	570 sh	640 sh
Ru2,4-D	340 sh	527	570 sh	640 sh
RuNAA	340 sh	525	570 sh	640 sh
[Ru$_2$Cl(μ-DAniF)$_3$(μ-O$_2$CMe)]	380 sh	511	594	690 sh
Ru'IAA	385 sh	498	594	690 sh
Ru'2,4-D	385 sh	478 sh	603	690 sh
Ru'NAA	360 sh	500	590	690 sh

[2] (a) Lin, C.; Ren, T.; Valente, E. J.; Zubkowski, J. D.; Smith, E. T. *Chem. Lett.* **1997**, *26* (8), 753–754. (b) Barral, M. C.; Herrero, S.; Jiménez-Aparicio, R.; Torres, M. R.; Urbanos, F. A. *Angew. Chem. Int. Ed.* **2005**, *44* (2), 305–307. (c) Chen, W.-Z.; Ren, T. *Organometallics* **2005**, *24* (11), 2660–2669. (d) Bear, J. L.; Han, B.; Huang, S.; Kadish, K. M. *Inorg. Chem.* **1996**, *35* (10), 3012–3021. (e) Castro, M. A.; Roitberg, A. E.; Cukiernik, F. D. *Inorg. Chem.* **2008**, *47* (11), 4682–4690.
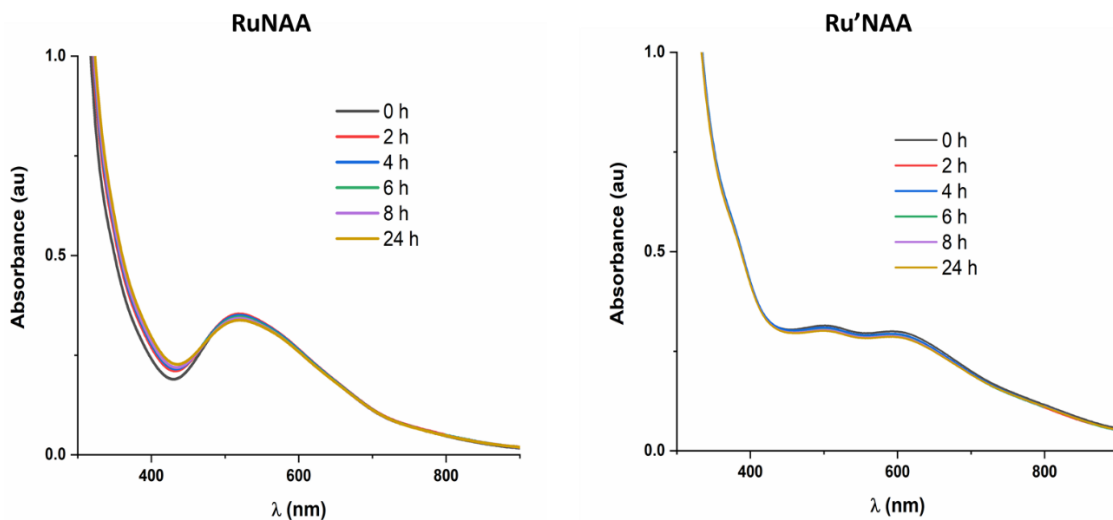
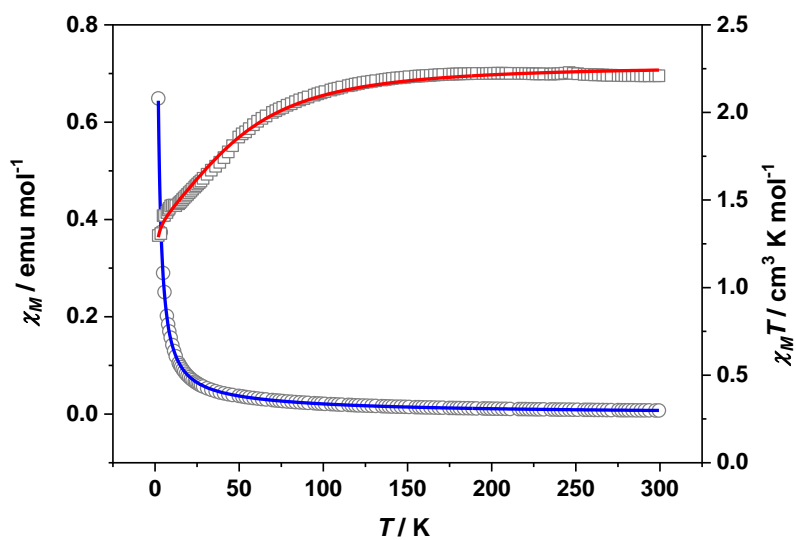**Figure S7**. Electronic spectra of **RuNAA** (left) and **Ru'NAA** (right) in DMSO/water solution using an HEPES KOH (4-(2-hydroxyethyl)-1-piperazineethanesulfonic acid) buffer at pH 6.5 over 24 h.
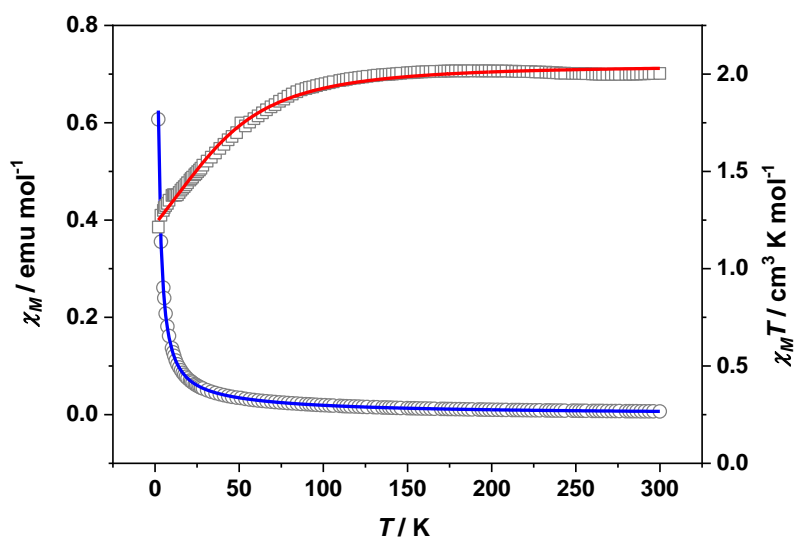
5. MAGNETIC MEASUREMENTS
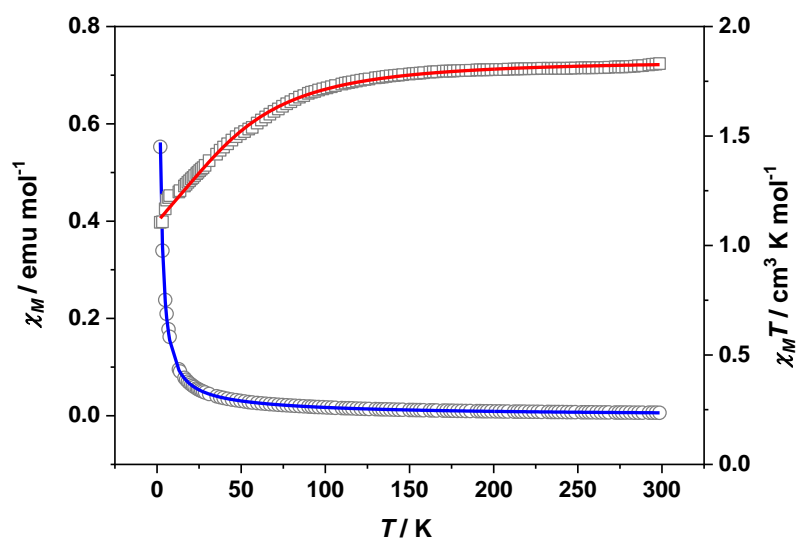
Figure S9. Temperature dependence of the molar susceptibility χ_M (circles) and $\chi_M \cdot T$ (squares) for **Ru'IAA**. Solid lines are the best fit to the data as described in the text.

Figure S10. Temperature dependence of the molar susceptibility χ_M (circles) and $\chi_M \cdot T$ (squares) for **Ru'2,4-D**. Solid lines are the best fit to the data as described in the text.

Figure S11. Temperature dependence of the molar susceptibility χ_M (circles) and $\chi_M \cdot T$ (squares) for **Ru'NAA**. Solid lines are the best fit to the data as described in the text.

Equations employed in the fitting of the magnetic data:

$$\chi_M = \frac{\chi_\parallel + 2\chi_\perp}{3}$$

Equation S1

$$\chi_\parallel = \left(\frac{Ng^2\beta^2}{k_BT}\right)\left[\frac{1 + 9\exp\left(-2D/k_BT\right)}{4\left(1 + \exp\left(-2D/k_BT\right)\right)}\right]$$

Equation S2

$$\chi_\perp = \left(\frac{Ng^2\beta^2}{k_BT}\right)\left[\frac{4 + \left(\frac{3k_BT}{D}\right)\left(1 - \exp\left(-2D/k_BT\right)\right)}{4\left(1 + \exp\left(-2D/k_BT\right)\right)}\right]$$

Equation S3

$$\chi_M{'} = \frac{\chi_M}{1 - \left(\frac{2zJ}{Ng^2\beta^2}\right)\chi_M}$$

Equation S4

(N, g, β, and k_B have their usual meanings)

6. BIOLOGICAL ASSAYS AND CHEMOMETRICS

**Table S7**. Multifactorial ANOVA.[3] Influence of pH and time on auxin activity.

2,4-D					
Source	Sum of squares	Df	Mean square	F-ratio	*p*-value
Main effects (pH)	0.0472109	2	0.0236054	115.81	0.0000
Main effect (time, h)	0.700818	2	0.350409	1710.06	0.0000
Interactions (pH-time)	0.0455153	4	0.0113788	55.82	0.0000
Ru2,4-D					
Source	Sum of squares	Df	Mean square	F-ratio	*p*-value
Main effects (pH)	0.0528029	2	0.0264014	20.19	0.0000
Main effect (time, h)	0.426837	2	0.213418	163.20	0.0000
Interactions (pH-time)	0.00732122	4	0.0183031	14.00	0.0000
Ru'2,4-D					
Source	Sum of squares	Df	Mean square	F-ratio	*p*-value
Main effects (pH)	0.0708965	2	0.0354482	202.64	0.0000
Main effect (time, h)	0.74159	2	0.370795	2119.69	0.0000
Interactions (pH-time)	0.0877365	4	0.02119341	125.39	0.0000
NAA					
Source	Sum of squares	Df	Mean square	F-ratio	*p*-value
Main effects (pH)	0.0659725	2	0.0329862	11.64	0.0009
Main effect (time, h)	0.804324	2	0.402162	141.90	0.0000
Interactions (pH-time)	0.060053	4	0.0150133	5.30	0.0073
RuNAA					
Source	Sum of squares	Df	Mean square	F-ratio	*p*-value
Main effects (pH)	0.0838757	2	0.041937	233.62	0.0000
Main effect (time, h)	0.355385	2	0.177692	989.84	0.0000
Interactions (pH-time)	0.0923937	4	0.0230984	128.67	0.0000
Ru'NAA					
Source	Sum of squares	Df	Mean square	F-ratio	*p*-value
Main effects (pH)	0.0734904	2	0.0367452	25.392	0.0000
Main effect (time, h)	0.416898	2	0.208449	144.03	0.0000
Interactions (pH-time)	0.0668784	4	0.0167196	11.55	0.0001

---

[3] C. Mongay Fernández, *Quimiometría*, UNIVERSITAT DE VALÈNCIA, 2014.
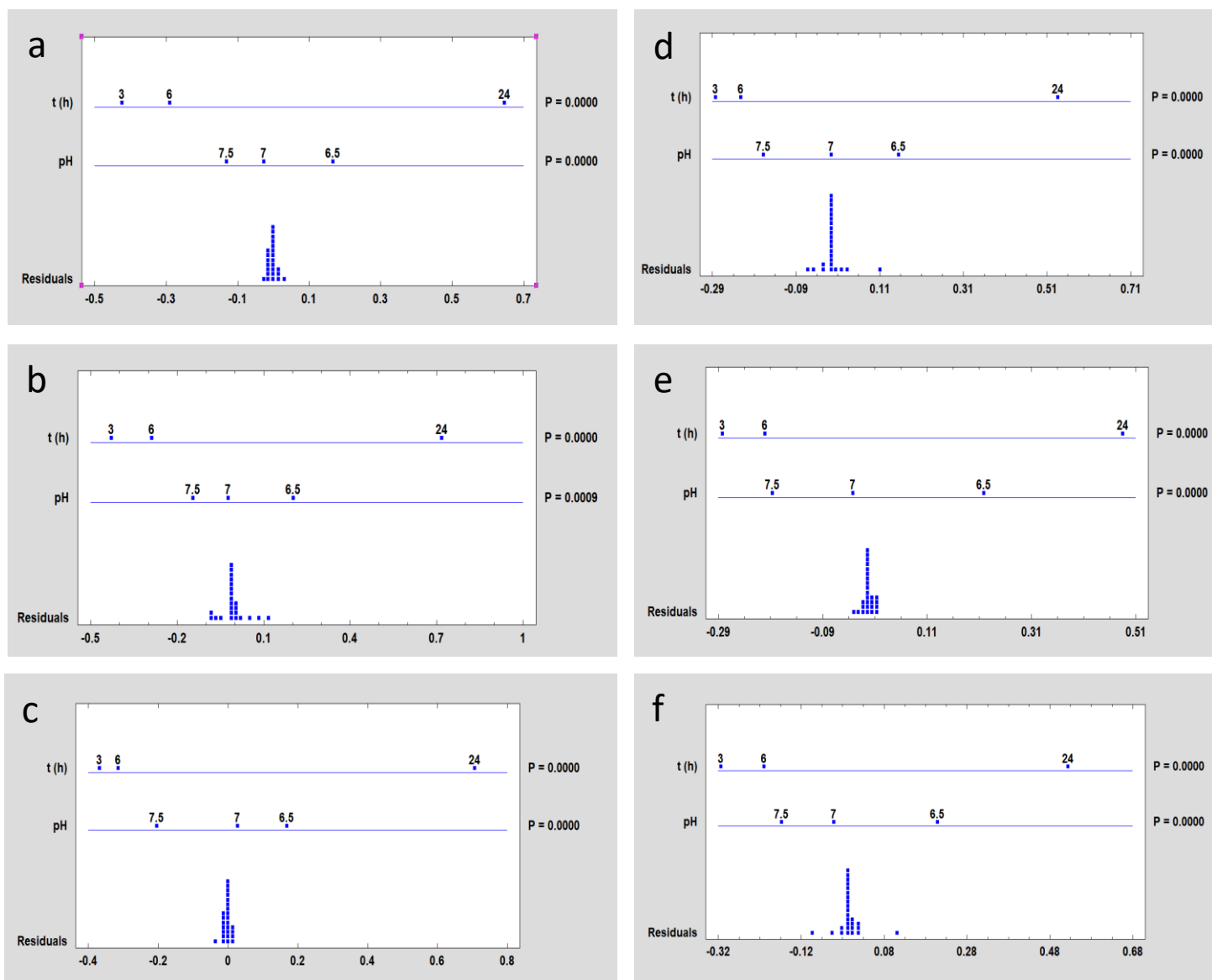
Figure S12. Multifactor ANOVA plots. Factors evaluated and *p*-values obtained. a) 2,4 D; b) **Ru2,4-D**; c) **Ru'2,4-D**; d) NAA; e) **RuNAA**; f) **Ru'NAA**.
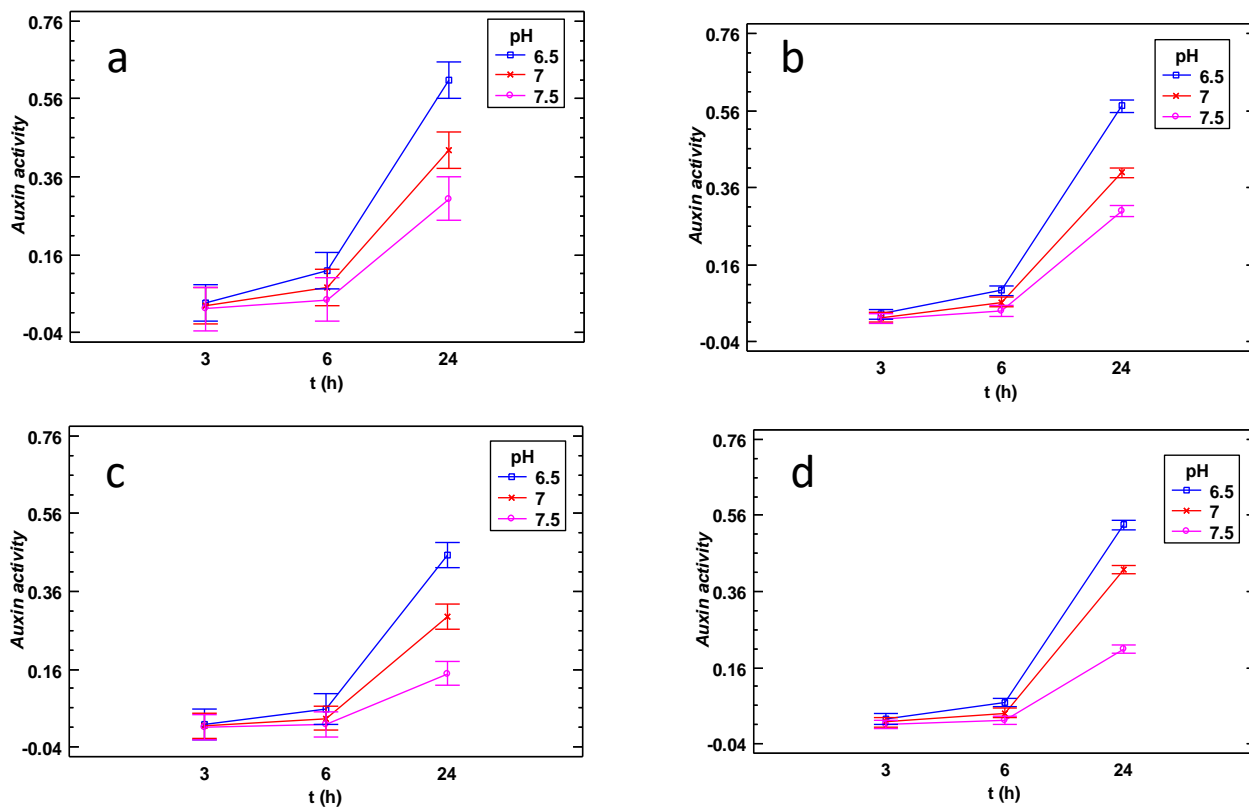
Figure S13. a) Variation of the auxin activity of NAA as a function of pH and time (the pH time cross-dependence is not observed for **RuNAA** and **Ru'NAA**). b) Variation of the auxin activity as a function of pH and time of 2,4-D. c) Variation of the auxin activity as a function of pH and time of **Ru2,4-D**. d) Variation of the auxin activity as a function of pH and time of **Ru'2,4-D**. Intervals have been estimated using the LSD statistic at 95% probability. Auxin activity is measured in 4-MU nmol·min^{-1}·µg^{-1} protein.